Available online at www.sciencedirect.com

ScienceDirect

Procedia Engineering 102 (2015) 346 – 355

Procedia Engineering

www.elsevier.com/locate/procedia

The 7th World Congress on Particle Technology (WCPT7)

# Synthesis of Zinc Carbonate Hydroxide Nanoparticles Using Microemulsion Process

Tamer Alhawi[a], Mohammad Rehan[a,b], David York[a], Xiaojun Lai[a]*

[a]*Institute of Particle Science and Engineering (IPSE), School of Process, Environmental and Materials Engineering (SPEME) University of Leeds, Leeds, LS2 9JT, UK*

[b]*Center of Excellence in Environmental Studies (CEES), King Abdulaziz University (KAU), Jeddah, Saudi Arabia*

**Abstract**

In order to control the particle size and morphology, zinc carbonate hydroxide $Zn_5(CO_3)_2(OH)_6$ nanoparticles have been synthesized using a reverse microemulsion technique. The pseudo-ternary phase diagrams of the two microemulsion systems, prepared using CTAB/1-butanol/n-octane/aqueous phase system with the aqueous phase comprised of either zinc nitrate ($Zn(NO_3)_2$) or sodium carbonate ($Na_2CO_3$), were experimentally constructed. The nanoparticles synthesized by mixing of the two emulsion systems were further characterized by X-ray diffraction (XRD), scanning electron microscopy (SEM) and thermogravimetric analysis (TGA). The nanoparticles were further characterized by X-ray diffraction (XRD), scanning electron microscopy (SEM) and thermogravimetric analysis (TGA). Several important experimental parameters have been investigated for the ability to control particle size and morphology as the function of water/surfactant molar ratio (ω), water/oil molar ratio (*S*) and the initial concentration of reactants in the aqueous phase. Results indicate that ω values have the ability to affect the particle size and levels of aggregation, while S values had no apparent effect. In addition, the initial concentration of reactants in the aqueous phase was considered to be an important parameter as raising its values from 0.1M to 0.5M produced an unknown phase of zinc carbonate, exhibiting larger particle size with a unique flake like morphology.


Selection and peer-review under responsibility of Chinese Society of Particuology, Institute of Process Engineering, Chinese Academy of Sciences (CAS)

*Keywords*: Zinc carbonate hydroxide, Nanoparticles, Microemulsion, CTAB, Phase diagram

* Corresponding author. Tel.: +44-113-343-2439; fax: +44-113-343-2384.
*E-mail address:* x.lai@leeds.ac.uk


Selection and peer-review under responsibility of Chinese Society of Particuology, Institute of Process Engineering, Chinese Academy of Sciences (CAS)
doi:10.1016/j.proeng.2015.01.158

## 1. Introduction

A microemulsion can be described as a thermodynamically stable system composed of an oil phase, aqueous phase, surfactant and sometimes a co-surfactant [1, 2]. Microemulsions have specific physical and chemical properties such as transparency, low viscosity, and homogeneity [2, 3]. Hence, since their discovery, several applications for microemulsions have been implemented in the industry which includes pharmaceutical drug delivery, enhanced oil recovery and nanoparticle synthesis [2, 4]. In today's industry, the search for particles with tailored size and morphology has become of increased interest as they may possess new more favored properties [5-7]. Among such compounds is zinc carbonate ($ZnCO_3$) which found its way as a useful substance in different sectors of the industry. Zinc carbonate has been used in respirators due to its effectiveness in removing toxic gases such as $SO_2$ and HCN [5, 8]. One other application of zinc carbonate – considered one of the most important – is the use as a precursor for the production of ultrafine zinc oxide (ZnO) particles. ZnO has numerous uses in the industry such as the use in electronics, solar cells, pigments and as an industrial catalyst [5-9].

Several zinc carbonate synthetic routes have been previously investigated and published in the literature. Zhang et al. (2004) synthesized zinc carbonate hydroxide ($Zn_5(CO_3)_2(OH)_6$) by direct precipitation of potassium carbonate ($K_2CO_3$) with zinc acetate ($Zn(CH_3COO)_2$) at room temperature [8]. Wu & Jiang (2006) were able to synthesize pure anhydrous $ZnCO_3$ nanocrystals by a solid-state reaction [6]. The experimental method consisted of grinding zinc sulphate heptahydrate ($ZnSO_4{\cdot}7H_2O$) and ammonium bicarbonate ($NH_4HCO_3$) in the presence of small amounts of polyethyleneglycol-octyl-phenylate (OP) surfactant at room temperature. Shamsipur et al. (2013) synthesized basic $ZnCO_3$ nanoparticles using direct precipitation of zinc nitrate heptahydrate ($Zn(NO_3)_2{\cdot}7H_2O$) and sodium carbonate ($Na_2CO_3$) [5]. Hu et al. (2010) synthesized hydrozincite ($Zn_5(CO_3)_2(OH)_6$) by utilizing a hydrothermal process between zinc acetate dihydrate ($Zn(CH_3COO)_2{\cdot}2H_2O$) and urea ($NH_2CONH_2$) [10]. Hingorani et al. (1993) synthesized zinc carbonate as a precursor for the production of ZnO using a microemulsion technique [11]. The authors utilized a CTAB/1-butanol/n-octane/aqueous phase system with the aqueous phase comprised of either zinc nitrate ($Zn(NO_3)_2$) or ammonium carbonate ($(NH_4)_2CO_3$).

In this research, the synthesis of zinc carbonate has been studied using a reverse microemulsion technique. The microemulsion system proposed by Hingorani et al. (1993) has been further investigated and the phase diagrams of zinc nitrate ($Zn(NO_3)_2$) and sodium carbonate ($Na_2CO_3$) are constructed. The as-synthesised particles are further characterized by XRD, SEM and TGA. Three important experimental parameters have been investigated herein for the ability to control particle size and morphology which are: water/surfactant molar ratio (ω), water/oil molar ratio (*S*) and the initial concentration of reactants in the aqueous phase.

## 2. Experimental

### *2.1. Zinc carbonate synthesis*

The preparation of zinc carbonate particles was carried out using a reverse microemulsion technique. The basic microemulsion system proposed by Hingorani et al. (1993) was utilized which consisted of Hexadecyltrimethyammonium bromide (CTAB, ≥98.0%; Sigma) as surfactant; 1-butanol (≥99.4%; Sigma-Aldrich) as co-surfactant; n-octane (≥98.0%; Sigma-Aldrich) as continuous oil phase. However, the dispersed aqueous phase in all our experiments consisted of a solution of known concentration of either zinc nitrate hexahydrate (≥99.0%; Sigma-Aldrich) or sodium carbonate (≥99.5%; Sigma-Aldrich). All reagents were used as purchased without further purification and deionized water was utilized in all experiments.

Stock solutions of known concentration of zinc nitrate hexahydrate and sodium carbonate were first freshly prepared to be used as aqueous phases in our study. The preparation of the microemulsions was performed in 250 ml conical flasks where the specified weights of CTAB, n-octane and 1-butanol were first added in this respective order. The resulting mixture was then shaken gently which resulted in the formation of a milky solution. The specified weight of aqueous phase from the respective stock solution was then added and the solution mixed with the help of a magnetic stirrer until a transparent, isotropic solution was observed. The first microemulsion "μE I" contained an aqueous phase of zinc nitrate hexahydrate while the second microemulsion "μE II" contained an aqueous phase of sodium carbonate.

The resulting two microemulsions were then combined and mixed in a 250 ml beaker with the help of a magnetic stirrer. The stirring was stopped when the appearance of the mixture turned from transparent (translucent in some cases) to cloudy which was indicative of the formation of precipitate. The contents of the beaker were then filtered using a Buckner-funnel connected to a pump. The filter paper used was 47 mm in diameter with 0.22 μm pore size. After filtration, the product was washed twice with 1:1 (v/v) solution of methanol and chloroform to get rid of all other microemulsion components. The as-prepared particles were then collected and dried overnight at 60 °C.

### *2.2. Phase diagram construction*

The phase diagrams of the proposed system were constructed using the titration method described in several publications [4, 12]. For this study, the phase diagrams were treated as a pseudo-ternary system in which the surfactant and co-surfactant were treated as one component. The ratio of surfactant to co-surfactant was fixed at 1:0.73 (w/w) as this particular ratio is able to maximize the solubility of certain aqueous solutions into stable microemulsions [13]. The titration method was carried out on 9 different compositions with an increment of 10% on the axis connecting the surfactant and oil vertices, however too high (>90% w/w) and too low (<10% w/w) surfactant compositions were not performed. All sample preparations were performed under room temperature which ranged from 32-33 °C.

### *2.3. Characterisation*

The X-ray powder diffraction (XRD; Bruker AXS D8 Advance) patterns of dried $ZnCO_3$ powder were recorded in the range of $8° \leq 2\theta \leq 75°$ with a Cu $K_\alpha$ source at 35 kV, 45 mA. High resolution surface images of the obtained $ZnCO_3$ nanoparticles were obtained using scanning electron microscopy (SEM; LEO 1530 Gemini). Thermogravimetric analysis (TGA; Mettler Toledo TGA/SDTA 851$^e$) was carried out on the dried powder in nitrogen atmosphere. The heating profile consisted of a steady increase in temperature at a rate of 10 °C/min from 30 to 480 °C, followed by maintaining isothermal conditions at 480°C for 10 minutes.

## 3. Results and discussion

The phase diagrams of CTAB/1-butanol/n-octane/aqueous phase system with the aqueous phase comprised of either 0.1 M sodium carbonate or 0.1 M zinc nitrate were constructed using the titration method and shown in Fig. 1 (a) and (b) respectively.

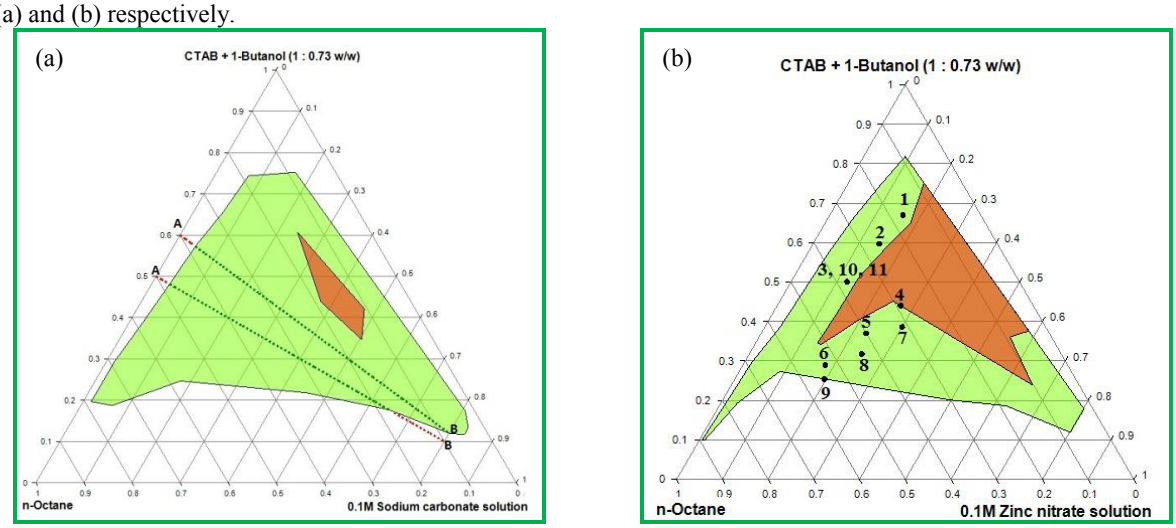


Fig. 1. Pseudo-ternary phase diagrams of (a) (CTAB+1-butanol)/n-octane/0.1 M sodium carbonate solution at 32-33 °C and (b) (CTAB+1-butanol)/n-octane/0.1 M zinc nitrate solution at 32-33 °C with the selected microemulsion compositions for this study.

To get a better understanding of the titration method, Fig. 1(a) demonstrates how each successive addition of an aqueous phase drop is accompanied by a movement along the dotted line from point A to point B. Therefore, the construction of the phase diagrams was performed as a result of visually inspecting microemulsion formation along such lines. A transparent, isotropic solution was considered a stable microemulsion while milky, turbid, gel-like, highly viscous and 2 or 3 phases were not considered microemulsions. The phase diagram using distilled water instead of an aqueous phase was not constructed for this study as it has already been thoroughly investigated by Ayyub et al. (1993) [13].

It can be seen from Fig. 1(a) that the phase diagram of CTAB/1-butanol/n-octane/ 0.1 M sodium carbonate system has the ability to form a wide range of stable microemulsions with varying compositions. Such compositions are represented in the figure by the green shaded area; on the other hand, the orange and white shaded areas represent compositions where no microemulsions formed. By referring to Fig. 1(a) and Fig. 1(b), it can be seen that 0.1 M sodium carbonate formed more stable microemulsions than 0.1 M zinc nitrate. Therefore, it was concluded that the choice of microemulsion compositions for this study would be restricted by microemulsion formation in the 0.1 M zinc nitrate phase diagram. Fig. 1(b) and Table 1 show the selected microemulsion compositions investigated in this study to assess the ability of microemulsion process as means of synthesising $ZnCO_3$ particles with controlled size and morphology distributions.

In the literature, several publications claim that microemulsion composition has a profound effect on the synthesised particle size and morphology [2, 14-16]. This is mainly due to the way microemulsion composition affects microemulsion droplet size. It is believed that the larger the droplet size the bigger the final particles are and vice versa [7, 16]. Hence, in the following study we chose two important microemulsion composition parameters with the highest likeliness to affect droplet size and ultimately particle size and morphology which are water/surfactant molar ratio (ω) and water/oil molar ratio (*S*).

To evaluate this effect, samples 1-9 were carefully selected from the constructed phase diagrams and their respective compositions can be found in Table 1. The choice of microemulsion compositions was restricted by the formation of stable microemulsions in the zinc nitrate phase diagram as it had a smaller area for stable microemulsion formation. Therefore, average ω values of 8.46, 21.64 and 27.10 and average *S* values of 5.98, 3.60 and 2.16 were chosen accordingly. The evaluation of the effect of ω values was achieved by varying ω values while keeping *S* values constant and vice versa.

Table 1. Summary of the selected microemulsion compositions investigated in this study.

| Sample No | Microemulsion composition (wt%) | | | Water/surfactant molar ratio (ω) | Water/oil molar ratio (*S*) | Aqueous phases molar ratio ($Zn:CO_3$)[a] |
|---|---|---|---|---|---|---|
| | n-octane | CTAB + 1-butanol | Aqueous phase | | | |
| 1 | 17.0 | 67.0 | 16.0 | 8.36 | 5.97 | 1.00 |
| 2 | 25.8 | 59.7 | 14.5 | 8.50 | 3.56 | 1.00 |
| 3 | 37.7 | 50.1 | 12.2 | 8.51 | 2.05 | 1.00 |
| 4 | 29.0 | 44.0 | 27.0 | 21.50 | 5.90 | 1.00 |
| 5 | 40.0 | 37.0 | 23.0 | 21.74 | 3.65 | 1.00 |
| 6 | 53.0 | 29.0 | 18.0 | 21.68 | 2.15 | 1.00 |
| 7 | 31.4 | 38.6 | 30.0 | 27.09 | 6.06 | 1.00 |
| 8 | 43.6 | 31.8 | 24.6 | 27.05 | 3.58 | 1.00 |
| 9 | 55.0 | 25.4 | 19.6 | 27.16 | 2.26 | 1.00 |
| 10 | 37.7 | 50.1 | 12.2 | 8.51 | 2.05 | 1.00 |
| 11 | 37.7 | 50.1 | 12.2 | 8.51 | 2.05 | 5.00 |

[a]Samples 1-9 had $[Zn(NO_3)_2] = [Na_2CO_3] = 0.1$ M; sample 10 had $[Zn(NO_3)_2] = [Na_2CO_3] = 0.5$ M; sample 11 had $[Zn(NO_3)_2] = 0.5$ M and $[Na_2CO_3] = 0.1$ M.

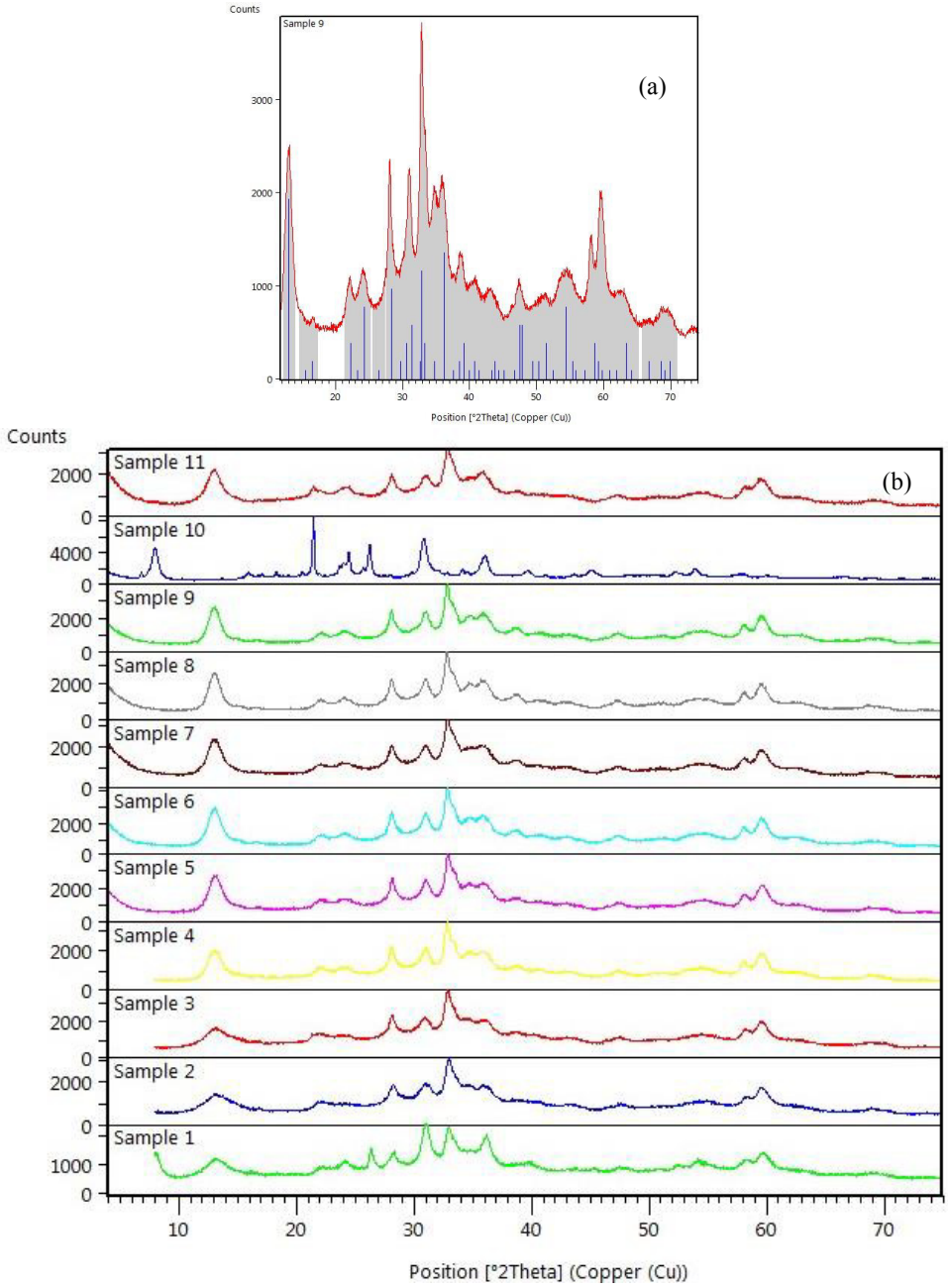


Fig. 2. XRD diffraction pattern of a typical sample matched with reference patterns in blue lines (a) 00-019-1458 and (b) XRD patterns for all samples 1-11.

The XRD patterns of the dried powder samples (1-11) are shown in Fig. 2. These patterns have been indexed using the reference data files from ICDD-PDF database. All 11 samples except sample 10 showed very similar XRD patterns with minor difference in some peak intensities, which could be attributed to the difference in crystallinity percentage and amount of amorphous contents of each sample. The best reference pattern matched with all samples

except sample 10 is the zinc carbonate hydroxide ($Zn_5(CO_3)_2(OH)_6$) also known as hydrozincite, card number No. 00-019-1458 (Fig 2(a)). However, some of the peaks seem to match better with reference pattern of zinc carbonate hydroxide hydrate ($Zn_4CO_3(OH)_6{\cdot}H_2O$), card No. 00-011-0287. This confirms that the particles produced are a mixture of ($Zn_5(CO_3)_2(OH)_6$) and ($Zn_4CO_3(OH)_6{\cdot}H_2O$), however ($Zn_5(CO_3)_2(OH)_6$) is present in larger quantities as evident by generating higher computer peak matching score during XRD pattern indexing.

The unusual sample 10 showed some extra peaks which did not match with any of the available zinc carbonate crystal structure in the ICDD database. These peaks are most probably formed due to the change in the overall zinc carbonate compound crystal structure or possibly due to the formation of a new phase. In this particular sample, the initial concentrations of both aqueous phases of zinc nitrate hexahydrate and sodium carbonate were raised from 0.1 M to 0.5 M, which resulted in the difference in crystal structure observed by XRD. It should be noted that the 0.5 M sodium carbonate microemulsion formed a translucent solution instead of a clear solution as obtained for all other samples using 0.1 M concentrations. Further investigation is needed to understand the effect of aqueous solution molar concentrations and ratios on the crystal structure, size and morphology.

Fig. 3 and 4 show the surface morphology of $Zn_5(CO_3)_2(OH)_6$ particles as in SEM images for samples 1-9. It can be seen that the individual nanoparticles generally exhibit spherical morphology with particle size ranging from 20-70 nm. To evaluate the effect of ω values on particle size and morphology, samples were compared in triplets where ω values were varied while *S* values were kept constant. For example, samples 1, 4 and 7 can be compared as they have a fixed average *S* value of 5.98, while average ω values varied from 8.36 to 21.50 to 27.09 respectively.

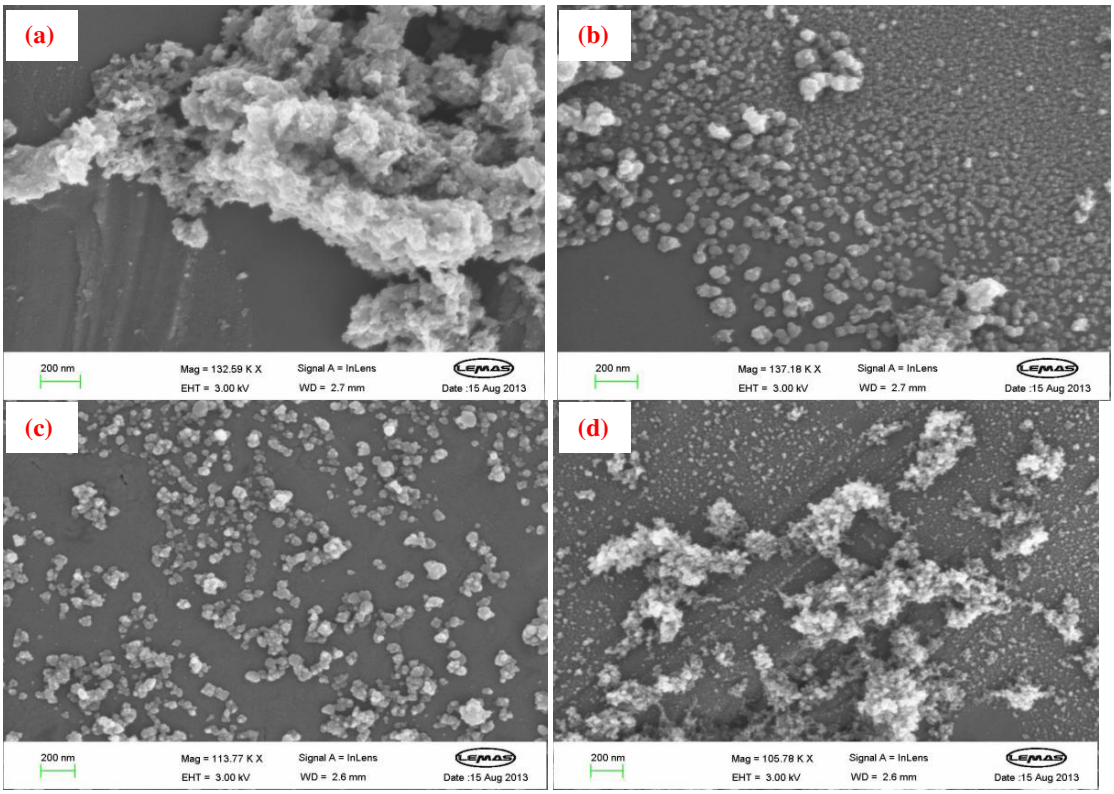

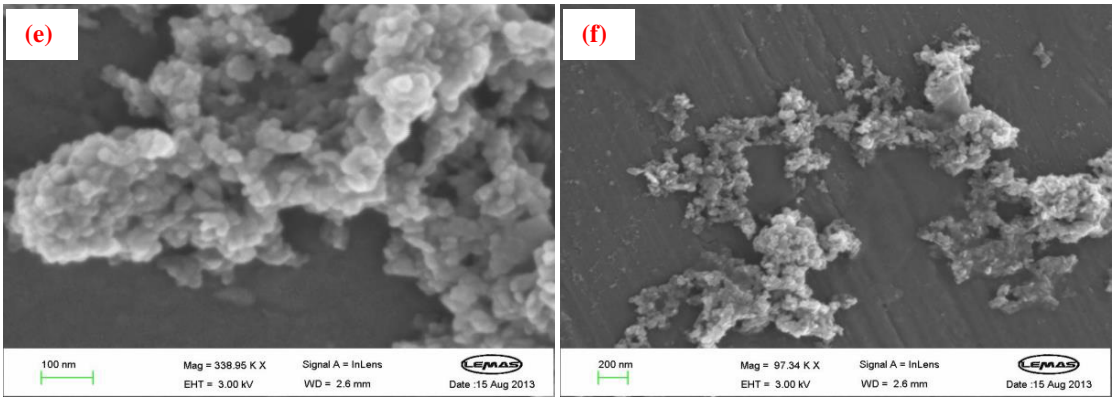


Fig. 3. SEM images of the obtained $ZnCO_3$ particles. (a) sample 1; (b) sample 2; (c) sample 3; (d) sample 4; (e) sample 5; (f) sample 6.

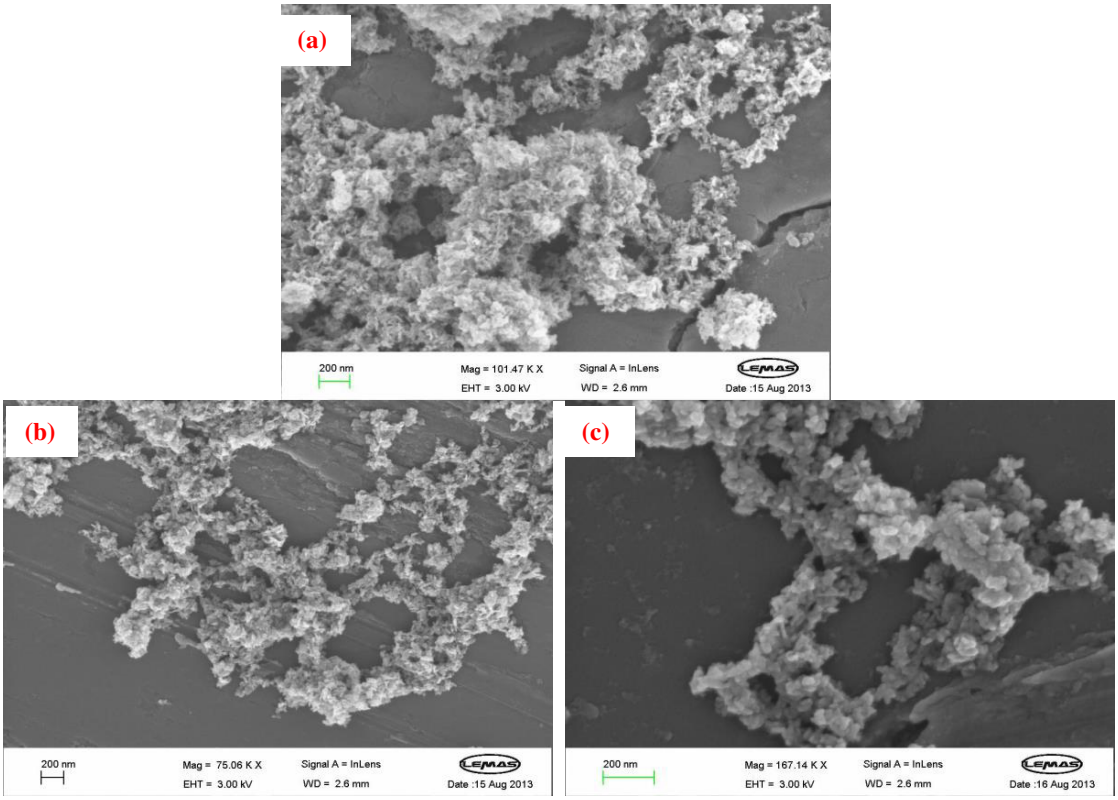


Fig. 4. SEM images of the obtained $ZnCO_3$ particles. (a) sample 7; (b) sample 8; (c) sample 9.

It can be clearly seen from Fig. 3 (b) that sample 2 showed minimal aggregation with scattered and well-defined spherical shaped particles. Nevertheless, we notice that as the average ω values were increased from 8.50 in sample 2 to 21.74 in sample 5 and 27.05 in sample 8, the phenomenon observed in sample 2 disappeared and the particles had larger aggregates with less defined morphology (Fig. 3 (e) and Fig. 4 (b)). This is because sample 2 has the highest surfactant content and lowest aqueous phase content when compared to samples 5 and 8. It is suggested that higher surfactant content will result in the formation of smaller more rigid droplets [14]. Consequently, as the

reactants start to nucleate and grow inside such droplets they will be restricted by the size and rigidity of the surfactant layer forming the droplets and hence produce homogenous particles with controlled size and morphology with minimal aggregation [16] as observed in SEM image of sample 2 (Fig. 3 (b)). Furthermore, as the water content is increased and the surfactant content is decreased in samples 5 and 8, the microemulsion droplets should theoretically become larger and less rigid [14,16] ultimately producing larger particles with higher levels of aggregation. A similar effect can be seen when comparing samples 3, 6 and 9. Hence, it can be concluded through SEM imaging that ω values have the ability to control the particle size and extent of aggregation. On the other hand, there seems to be no apparent effect on particle size and morphology associated with varying *S* values.

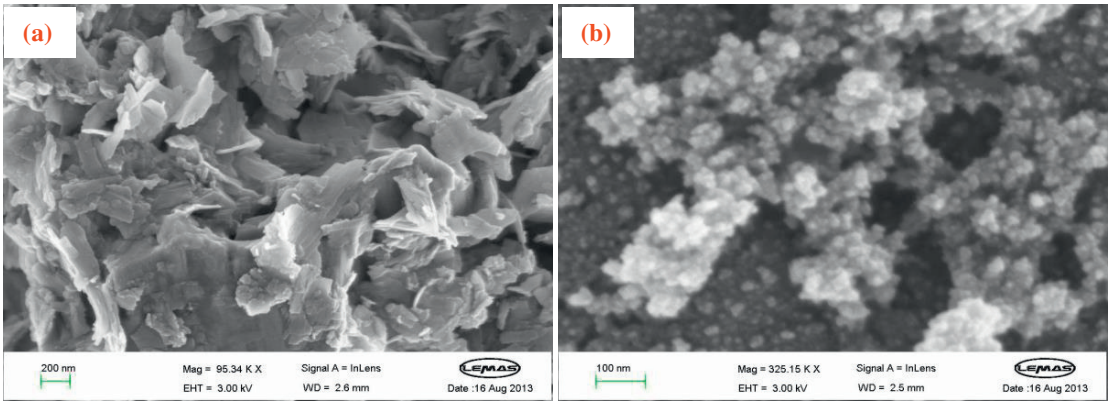


Fig. 5. SEM images of the obtained $ZnCO_3$ particles. (a) sample 10; (b) sample 11.

Another experimental parameter with high likeliness to have an effect on particle size and morphology is the initial concentration of reactants in the microemulsion's aqueous phase. Several publications have shown evidence that this parameter has a profound effect of particle size and morphology [2, 3, 15, 16]. Therefore, the evaluation of this effect was carried out through samples 3, 10 and 11, where microemulsion composition was kept constant and the initial concentrations of the reactants were changed. Sample 3 had 0.1 M $Zn(NO_3)_2$ and 0.1 M $Na_2CO_3$; sample 10 had 0.5 M $Zn(NO_3)_2$ and 0.5 M $Na_2CO_3$; and sample 11 had 0.5 M $Zn(NO_3)_2$ and 0.1 M $Na_2CO_3$.

Fig. 3 (c), Fig. 5 (a) and (b) show the surface morphologies of samples 3, 10 and 11 respectively. When the initial concentration of both reactants was 0.1 M in sample 3, we observed scattered and well-defined spherical particles (Fig. 3 (c)). However, as the initial concentration of both reactants was raised to 0.5 M in sample 10, we observed a drastic change in particle size and morphology (Fig. 5 (a)). The morphology changed from the well-defined spherical shaped particles to irregular flake-like particles. Moreover, the morphology change was accompanied by an increase in particle size from approximately 50 nm to about 400 nm flakes. This might be an indication that the droplet size has risen remarkably as a result of an increase in surfactant layer fluidity leading to the formation of bigger and coarser particles [2, 3]. The unique flake like morphology of particles can also be correlated to the unknown crystal phase of zinc carbonate noticed in XRD pattern of this particular sample 10. As for sample 11, we observed that the particles were produced again in spherical shaped morphology as observed in previous samples, however, the degree of aggregation is very high (Fig. 5 (b)). In conclusion, results have shown that the initial concentration of the reactants in the aqueous phase does in fact play a significant role in influencing the particle's phase, size, morphology and extent of aggregation.

Samples 1-9 were further analysed by TGA. The decomposition process of $Zn_5(CO_3)_2(OH)_6$ and $Zn_4CO_3(OH)_6{\cdot}H_2O$ to form zinc oxide (ZnO) can be illustrated by reactions (1) and (2) below [9, 17, 18], with theoretical percentage mass loss of 25.9 % and 25.2 % respectively.

$$Zn_5(CO_3)_2(OH)_6 \rightarrow 5ZnO + 2CO_2 + 3H_2O \quad (1)$$

$$Zn_4CO_3(OH)_6 \cdot H_2O \rightarrow 4ZnO + CO_2 + 4H_2O \quad (2)$$

Fig. 6(a) shows the TG curve obtained from sample 1 and is representative of samples 1-9 and 11. As expected, a characteristic single-step decomposition process between approximately 180 °C and 350 °C is observed, in which $Zn_5(CO_3)_2(OH)_6$ and $Zn_4CO_3(OH)_6{\cdot}H_2O$ decompose to form ZnO with the release of $CO_2$ and $H_2O$. The calculated percentage mass loss from Fig. 6(a) was 26.2% which is comparable to the theoretically calculated values.

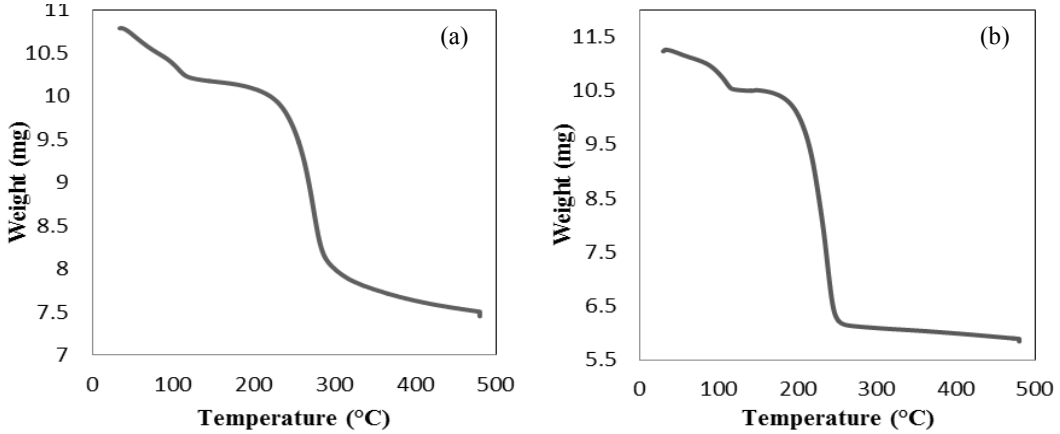


Fig. 6. Thermogravimetric curve (a) sample 1 and (b) sample 10.

To further confirm the change in phase observed in the XRD pattern of sample 10, TGA analysis was performed and the TG curve can be seen in Fig. 6(b). It was thought that the percentage weight loss of sample 10 would be higher than the theoretically calculated ones as a result of different phase and morphology of particles observed by XRD and SEM analysis respectively. This was true as the percentage weight loss of this particular sample was found to be 42.2% which is significantly higher than the values calculated theoretically and the values obtained from all other samples studied herein. Nevertheless, the same one-step decomposition process is observed between approximately 190 – 250 °C.

## 4. Conclusion

Zinc carbonate hydroxide ($Zn_5(CO_3)_2(OH)_6$) nanoparticles have been successfully synthesized using a reverse microemulsion technique. Prior to particle synthesis, the pseudo-ternary phase diagrams of the proposed CTAB/1-butanol/n-octane/aqueous phase system with the aqueous phase comprised of either $Zn(NO_3)_2$ or $Na_2CO_3$ were constructed. Several important experimental parameters have been investigated for the ability to control particle size and morphology such as water/surfactant molar ratio (ω), water/oil molar ratio (*S*) and the initial reactant concentration in the aqueous phase. XRD analysis revealed that microemulsion composition had no effect on the chemistry behind the precipitation reaction; however, raising the initial concentration of the reactants in the aqueous phase from 0.1 M to 0.5 M produced an unknown phase of zinc carbonate. The particles from this phase exhibited larger size and unique flake-like morphology as opposed to the smaller spherical shaped particles obtained from all other samples studied. Furthermore, the intensity of the diffraction peaks from most samples seems to be quite low with high background indicating the presence of a significant amount of amorphous content. SEM images revealed that the particles produced from most of the samples studied generally exhibit spherical morphology with particle size ranging from 20-70 nm. It is also observed from these images that ω values have the ability to control the particle size and extent of aggregation, while *S* values had no apparent effect on particle size and morphology. TGA analysis of all the samples studied showed the typical single-step decomposition process to form ZnO. The percentage weight loss values of all the samples, excluding sample 10, were similar to the theoretically calculated ones. Sample 10 showed a value significantly higher which is attributed to the different phase structure and morphology observed by XRD and SEM. Overall it has been demonstrated that the microemulsion process has the potential to synthesise zinc carbonate nanoparticles with controlled size and morphology distributions.

## Acknowledgements

The authors wish to extend their gratitude for the Institute of Particle Science and Engineering (IPSE) at the University of Leeds for providing all the facilities, equipment and their financial support.

## References

[1] P. Kumar, K. Mittal, Handbook of Microemulsion Science and Technology. New York: CRC Press, 1999.
[2] M. A. Malik, M. Y. Wani, M. A. Hashim, Microemulsion method: A novel route to synthesize organic and inorganic Nanomaterials, Arab. J. of Chem. 5 (2012) 397–417.
[3] J. Eastoe, M. J. Hollamby, L. Hudson, Recent advances in nanoparticle synthesis with reversed micelles, Adv. in col. and Interf. Sci. 128-130 (2006), 5–15.
[4] X. Jian, L. Ganzuo, Z. Zhiqiang, Z. Guowei, J. Kejian, A study of the microstructure of CTAB/1-butanol/octane/water system by PGSE-NMR, conductivity and cryo-TEM, Coll. and Surf. A: Physicochem. and Eng. Asp. 191 (2001) 269–278.
[5] M. Shamsipur, S. M. Pourmortazavi, S. S. Hajimirsadeghi, M. M. Zahedi, M. R. Nasrabadi, Facile synthesis of zinc carbonate and zinc oxide nanoparticles via direct carbonation and thermal decomposition, Cera. Internat. 39 (2013) 819–827.
[6] W. Wu, Q. Jiang, Preparation of nanocrystalline zinc carbonate and zinc oxide via solid-state reaction at room temperature, Mater. Let. 60 (2006)., 2791–2794.
[7] M. Winkelmann, E.-M.Grimm, T. Comunian, B. Freudig, Y. Zhou, W. Gerlinger, H. P. Schuchmann, Controlled droplet coalescence in miniemulsions to synthesize zinc oxide nanoparticles by precipitation. Chem. Eng. Sci. 92 (2013) 126–133.
[8] S. Zhang, H. Fortier, J. R. Dahn, Characterization of zinc carbonate hydroxides synthesized by precipitation from zinc acetate and potassium carbonate solutions, Mater. Res. Bull. 39 (2004) 1939–1948.
[9] K. Kakiuchi, M. Saito, S. Fujihara, Fabrication of ZnO films consisting of densely accumulated mesoporous nanosheets and their dye-sensitized solar cell performance, Thin Sol. Fil. 516 (2008) 2026–2030.
[10] S.-H. Hu, Y.-C. Chen, C.-C. Hwang, C.-H. Peng, D.-C. Gong, Analysis of growth parameters for hydrothermal synthesis of ZnO nanoparticles through a statistical experimental design method, J. of Mater. Sci. 45 (2010) 5309–5317.
[11] S. Hingorani, V. Pillai, P. Kumar, M. S. Multani, D. O. Shah, Microemulsion Mediated Synthesis of Zinc-Oxide Nanoparticles for Varistor Studies, Mater. Res. Bull. 28 (1993) 1303–1310.
[12] T. Schmidts, P. Nocker, G. Lavi, J. Kuhlmann, P. Czermak, F. Runkel, Development of an alternative, time and cost saving method of creating pseudoternary diagrams using the example of a microemulsion, Coll. and Surf. A: Physicochem. and Eng. Asp. 340 (2009) 187–192.
[13] P. Ayyub, A. Maitra, D. Shah, Microstructure of the CTAB-Butanol-Octane-Water Microemulsion System: Effect of Dissolved Salts, J. of the Chem. Soc. Farad. Transac. 89 (1993) 3585–3589.
[14] F. Rauscher, P. Veit, K. Sundmacher, Analysis of a technical-grade w/o-microemulsion and its application for the precipitation of calcium carbonate nanoparticles, Coll. and Surf. A: Physicochem. and Eng. Asp. 254 (2005) 183–191.
[15] C. Y. Tai, C. Chen, Particle morphology, habit, and size control of CaCO3 using reverse microemulsion technique, Chem. Eng. Sci. 63 (2008) 3632–3642.
[16] I. Capek, Preparation of metal nanoparticles in water-in-oil (w/o) microemulsions, Advan. in coll. and inter. Sci. 110 (2004) 49–74.
[17] Z. Li, X. Shen, X. Feng, P. Wang, Z. Wu, Non-isothermal kinetics studies on the thermal decomposition of zinc hydroxide carbonate, Thermochimica Acta, 438 (2005) 102–106.
[18] M. Bitenc, M. Marinsek, Z. C. Orel, Preparation and characterization of zinc hydroxide carbonate and porous zinc oxide particles, J. of Euro. Cera. Soc. 28 (2008) 2915–2921.